Analysis of land subsidence caused by groundwater overexploitation in the Gediz River Basin based on Sentinel-1 observations

María Navarro-Hernández[1], Roberto Tomás[1], Javier Valdes-Abellan[1], Guadalupe Bru[2], Pablo Ezquerro[2], Carolina Guardiola-Albert[2], Alper Elçi[3], Elif Aysu Batkan[3], Baris Caylak[3], Ören Ali Hakan[3], Claudia Meisina[4], Laura Pedretti[4], and Michelle Rygus[4]   email: mainnahe@ua.es

Introduction

Land subsidence due to groundwater withdrawal is one of the most extensive types of geological phenomenon induced by human activity in the 20th century, affecting many principal cities and regions in the world (Herrera-García et al., 2021). The differential interferometric synthetic aperture radar (DInSAR) technology has been developed and widely applied for earth observation with millimetre level precision and wide spatial coverage under all weather conditions with minimal cloud and rainfall affections (Sadeghi et al., 2021).

Study area

The Gediz River Basin is a tectonic valley located in western Turkey and developed from the regional extension horst-graben systems (**Figure 1**.). Groundwater being the main supplying source for agricultural and household water demand, the interaction between these human activities and the natural features gives rise to the pressure on the quantity and quality of water resources, positioning the Gediz Valley as one of the most stressed basins in the country (Duru et al., 2018; Elçi et al., 2015). Regional tectonics also play an important role in the towns of the valley. The noteworthy reason is because some important towns are built over some active faults placed in the southern margin of the basin (e.g. Alaşehir and Sarıgöl), where the graben presents more seismic activity and the highest earthquake record (F. Poyraz et al., 2019).
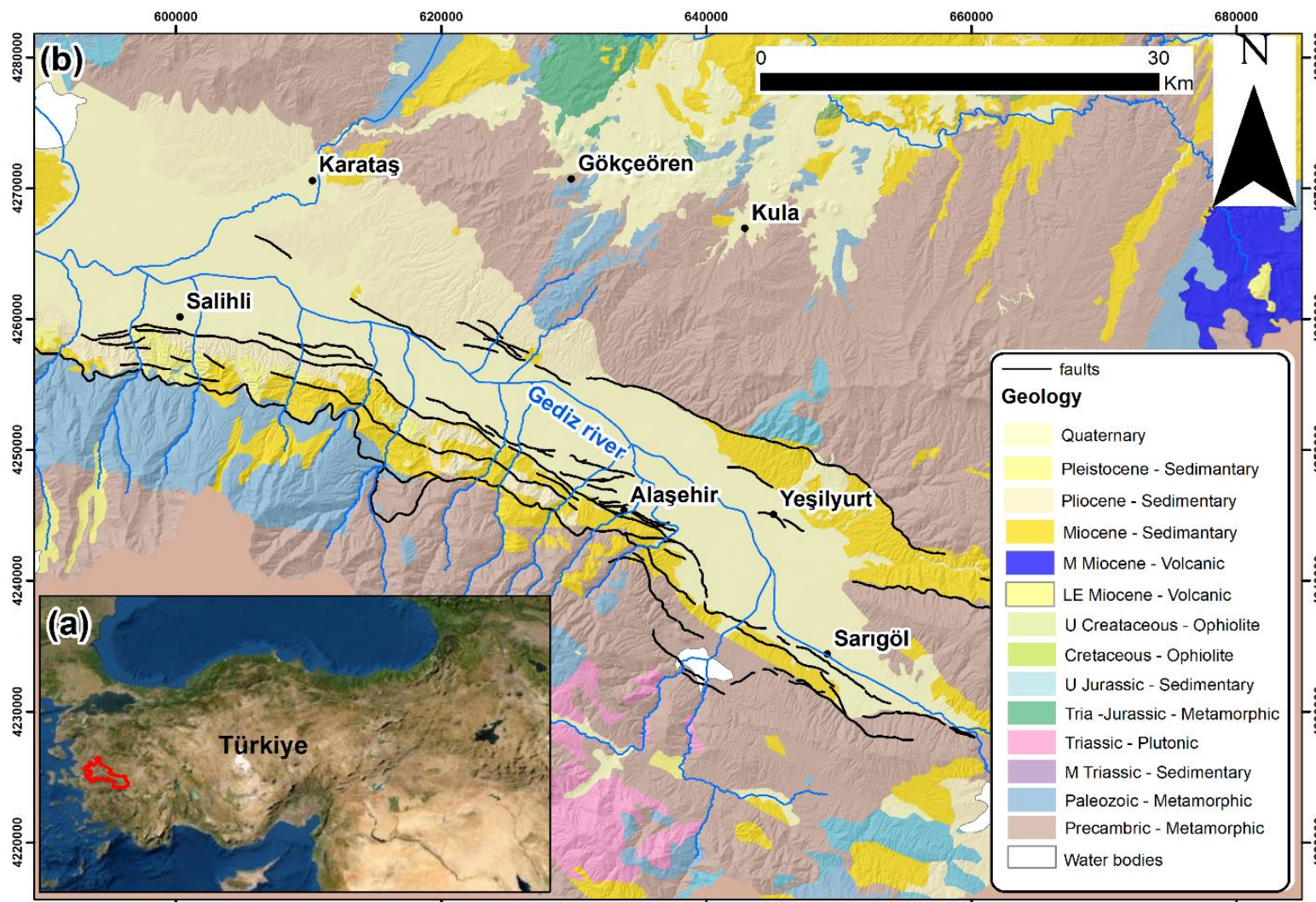

Figure 1. . (a) Location of the GRB (red polygon). (b) Geological map of the study area with delineation of regional faults.
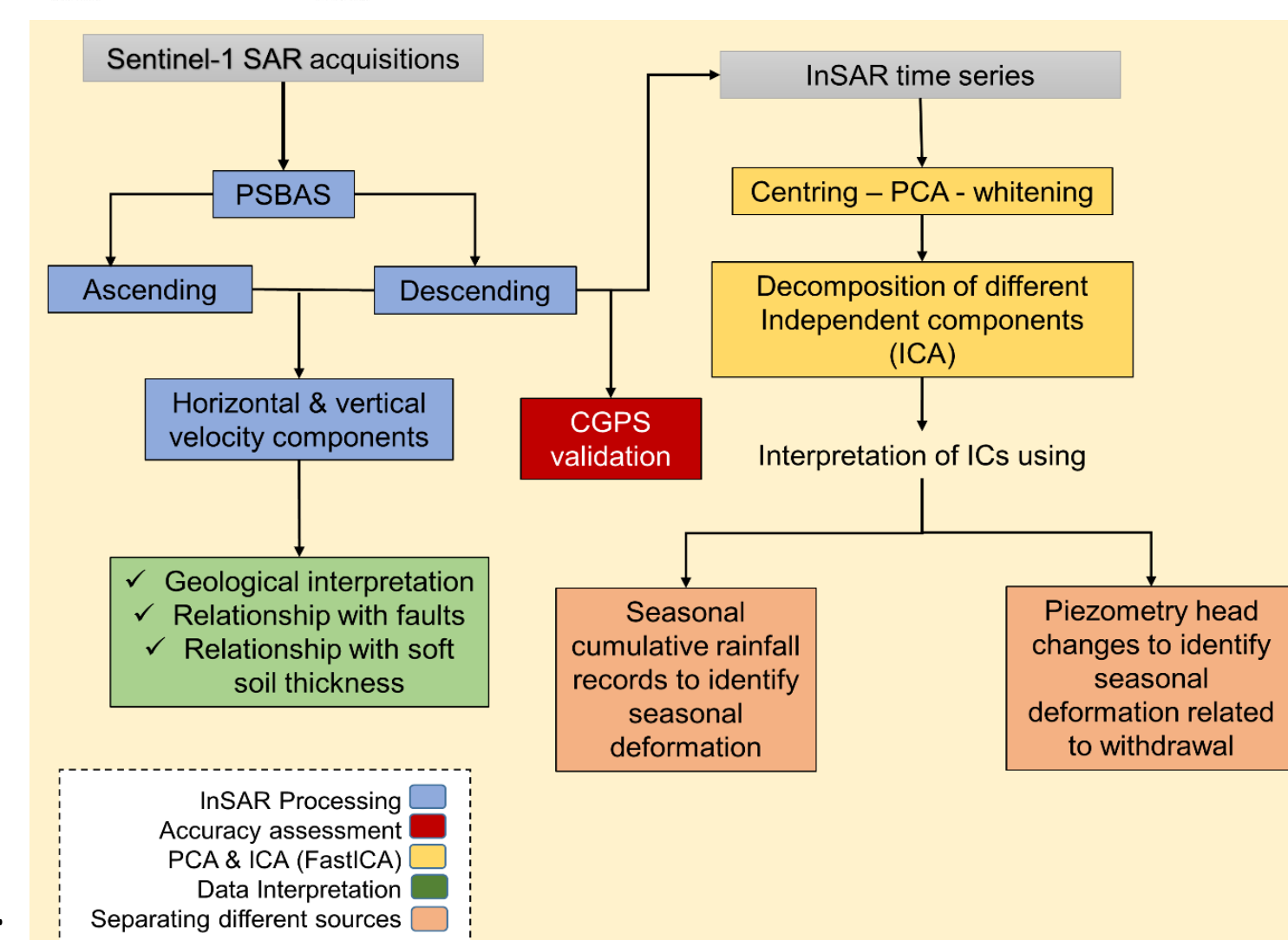
Methods

The aim of this paper is to evaluate the role of tectonic activity and groundwater withdrawal on land subsidence, and to investigate the influence of other trigger factors such as faults and soft soil thickness layers. For this purpose, the P-SBAS algorithm was applied using 98 and 123 Sentinel-1 SAR images in ascending and descending orbits, respectively, from 2016 to 2020. Subsequently, an Independent Component Analysis was applied to the InSAR time series in order to separate spatiotemporal patterns of long-term deformation and seasonal variations (**Figure 2**).
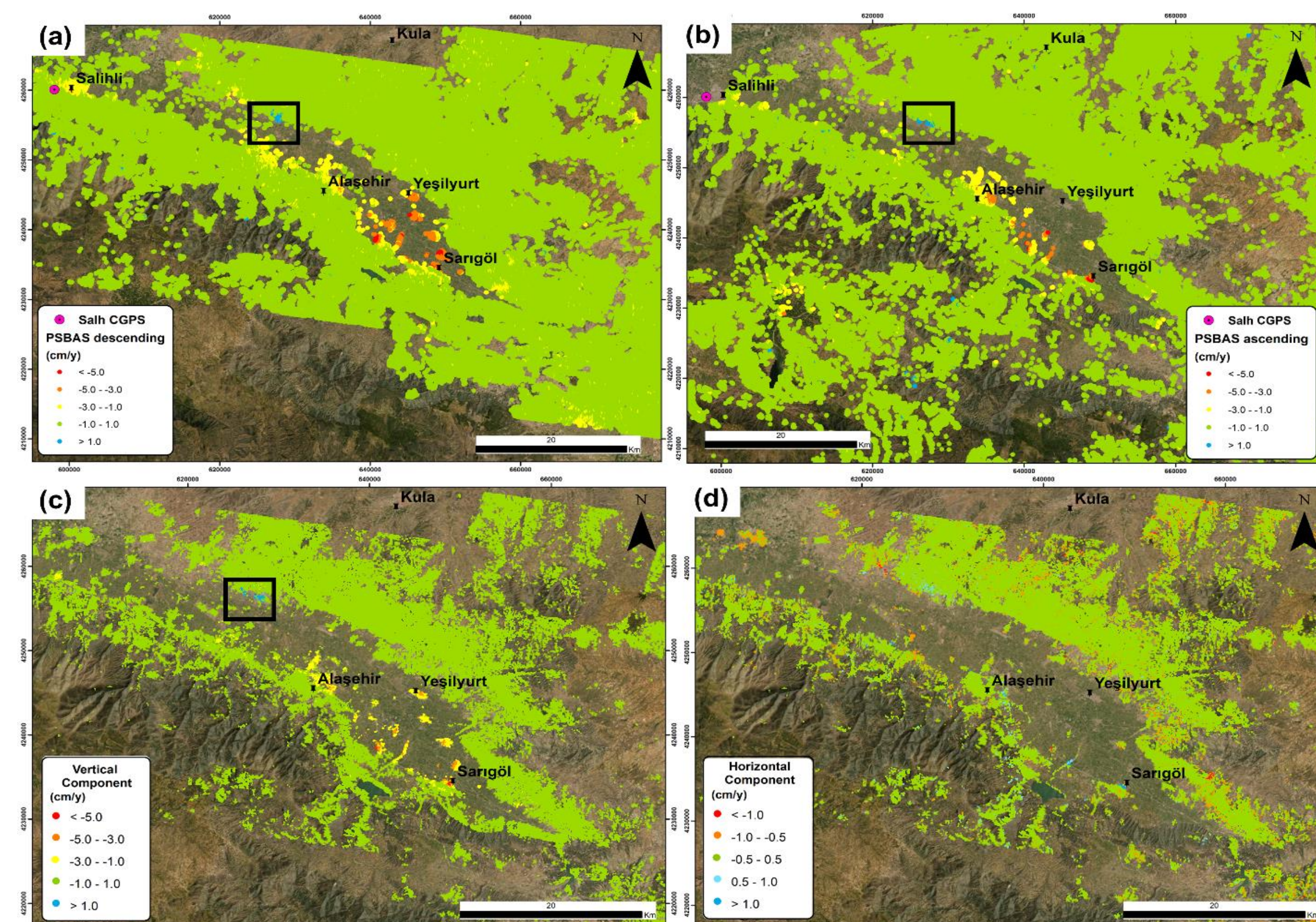
Results & Discussion

Figure 3. . P-SBAS displacement rate and SALH CGPS location. (a) LOS displacement rates for descending orbit, (b) LOS displacement rates for ascending orbit, (c) vertical displacement rates, V_U; and (d) east-west horizontal displacement rates, V_E.

Peak LOS rates within the limits of the study area have a similar range, varying from **-6.37** to **1.84 cm/year** for the descending orbit and from **-6.40** to **2.87 cm/year** for the ascending (**Figure 3**.). Results were validated by the ValInSAR code obtaining a "High Accuracy" result (R²=0.91; RMSE=0.91).

The distribution of the soft soil thickness is shown in **Figure 4a**. There is evidence of some agreements between high soft soil thickness and the highest displacement areas detected by InSAR located to the east and in the centre of the valley (red circle in **Figure 4a and 4b**). The correlation plot exhibits a good agreement between both variables with a R² of 0.853. Additionally, in **Figure 5**. IC1 explains the 96% of the eigenvectors and its signal has a similar spatial distribution as the LOS deformation rate map. The positive IC1 score values (**Figure 5a**.) can be correlated to the increase of clay material thickness, mainly accumulated in the centre of the basin.

Figure 2. Flowchart of the methodology applied in this work.

Figure 6 suggests that the decline in groundwater levels mainly occurs in the centre of the basin due to the agriculture activity and also in the southern border where the largest towns in the area are located (i.e., Salihli, Alaşehir and Sarıgöl). Comparing this information with the IC2 score map in **Figure 6d** it can be seen that they are in agreement and that the distribution of IC2 overlaps in some areas with the IC1 extent, suggesting that aquitard layer compaction can be related to the groundwater extraction.

Aligned structures have been detected in the study area by the Sentinel-1 satellite and they agree with the mapped active faults, as can be seen in Sarıgöl fault (**Figure 7a**). In this area the thickness of the clay and silty material changes drastically on either side of the fault due to the topography of the bedrock causing a differential compaction and, as a consequence, important structural damage in the city (**Figures 7c-d**).
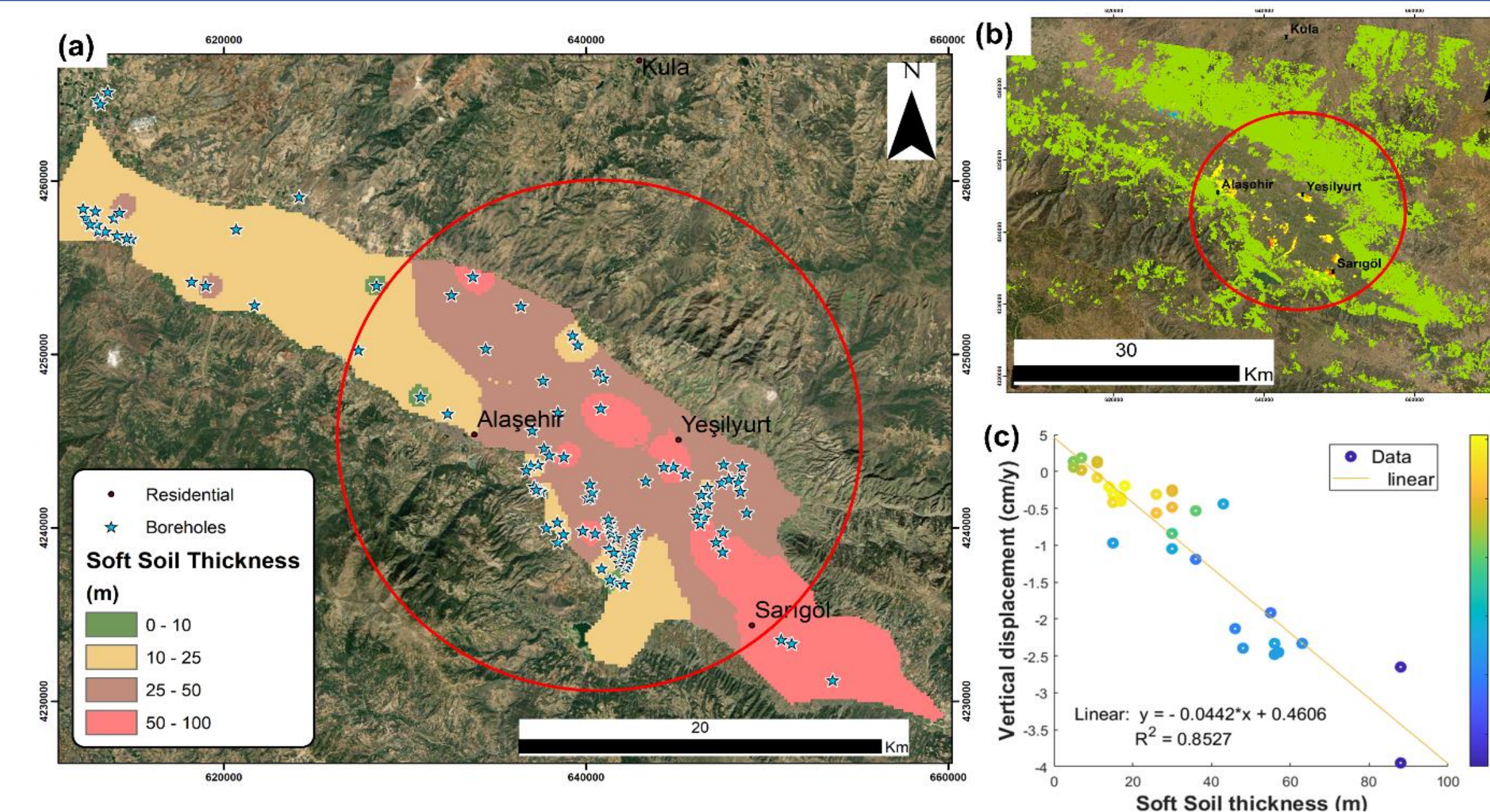

Figure 4. Relationship between soft soil thickness and land subsidence: (a) Soft soil thickness map derived from boreholes. (b) Vertical component of LOS displacement rate. (c) Correlation plot between soft soil thickness and vertical displacement rate.
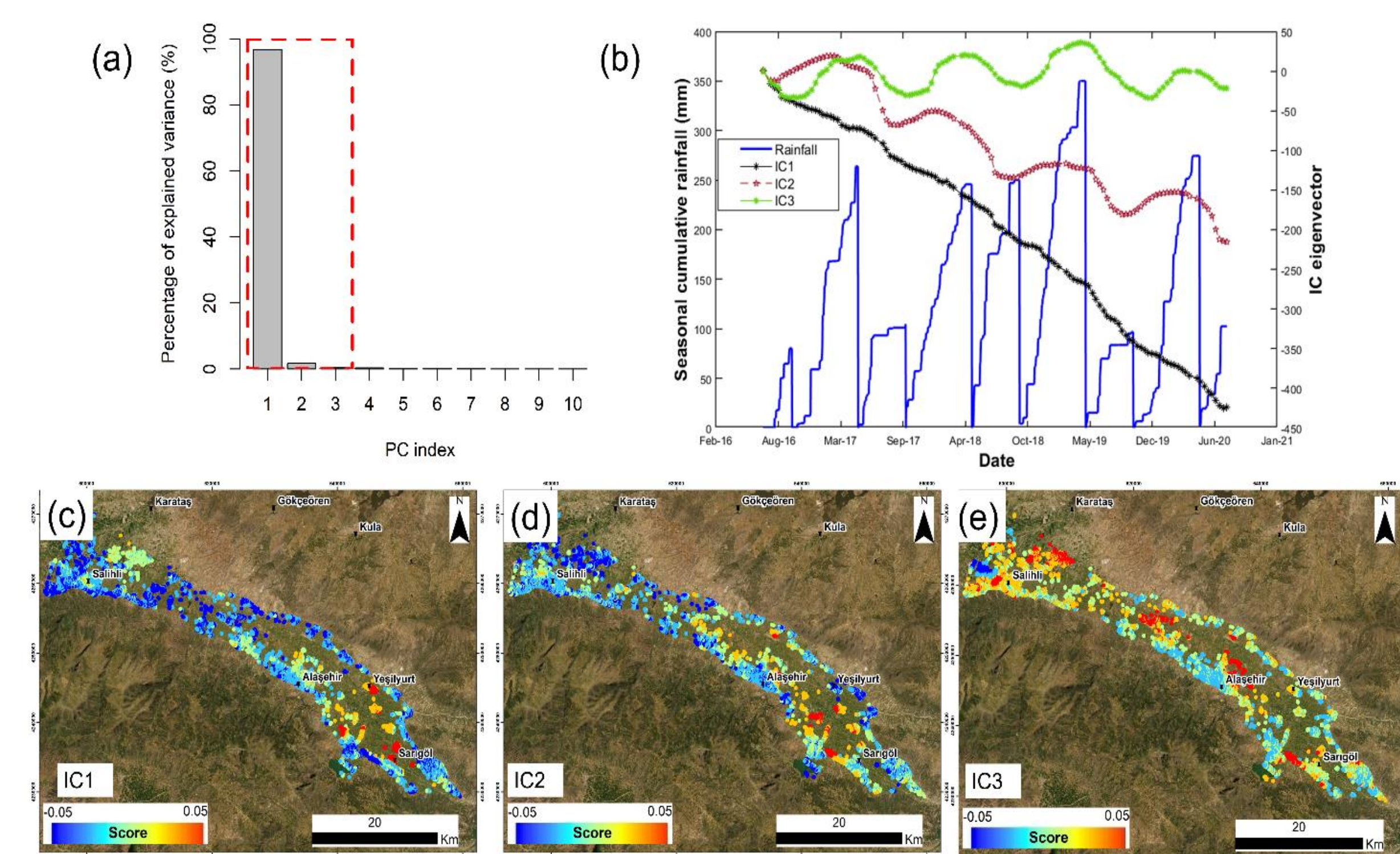

Figure 5. FastICA results: (a) Variance explained by each component in PCA, (b) ICs eigenvector time series compared with seasonal cumulative rainfall (blue), (c) IC1 score map, (d) IC2 score map, (e) IC3 score map.
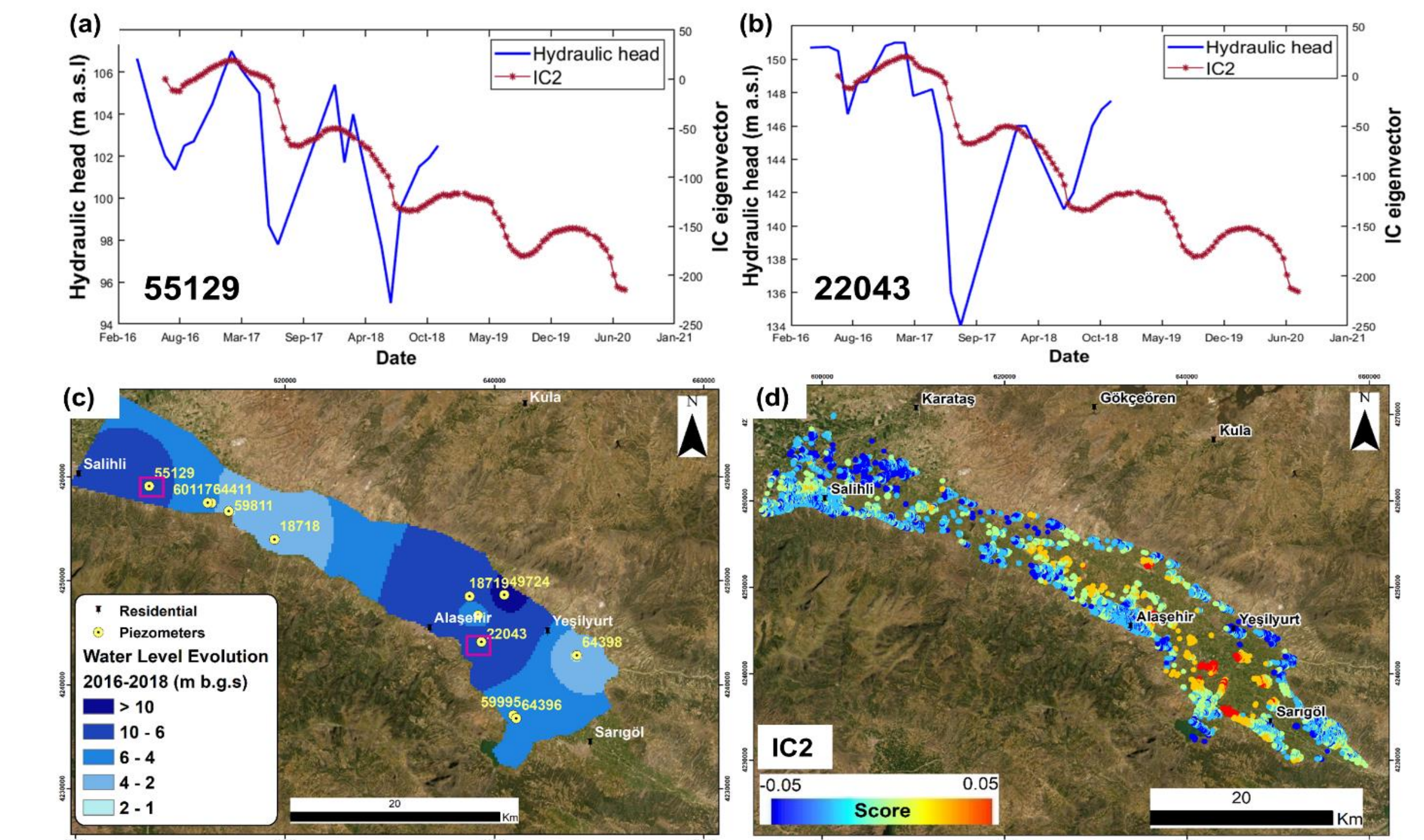

Figure 6. Relationship between seasonality and piezometric head evolution: (a) IC2 and piezometric head time series at the well 55129. (b) IC2 and piezometric head time series at the well 22043, (c) spatial distribution of groundwater level evolution from 2016 to 2018 and (d) IC2 map score.
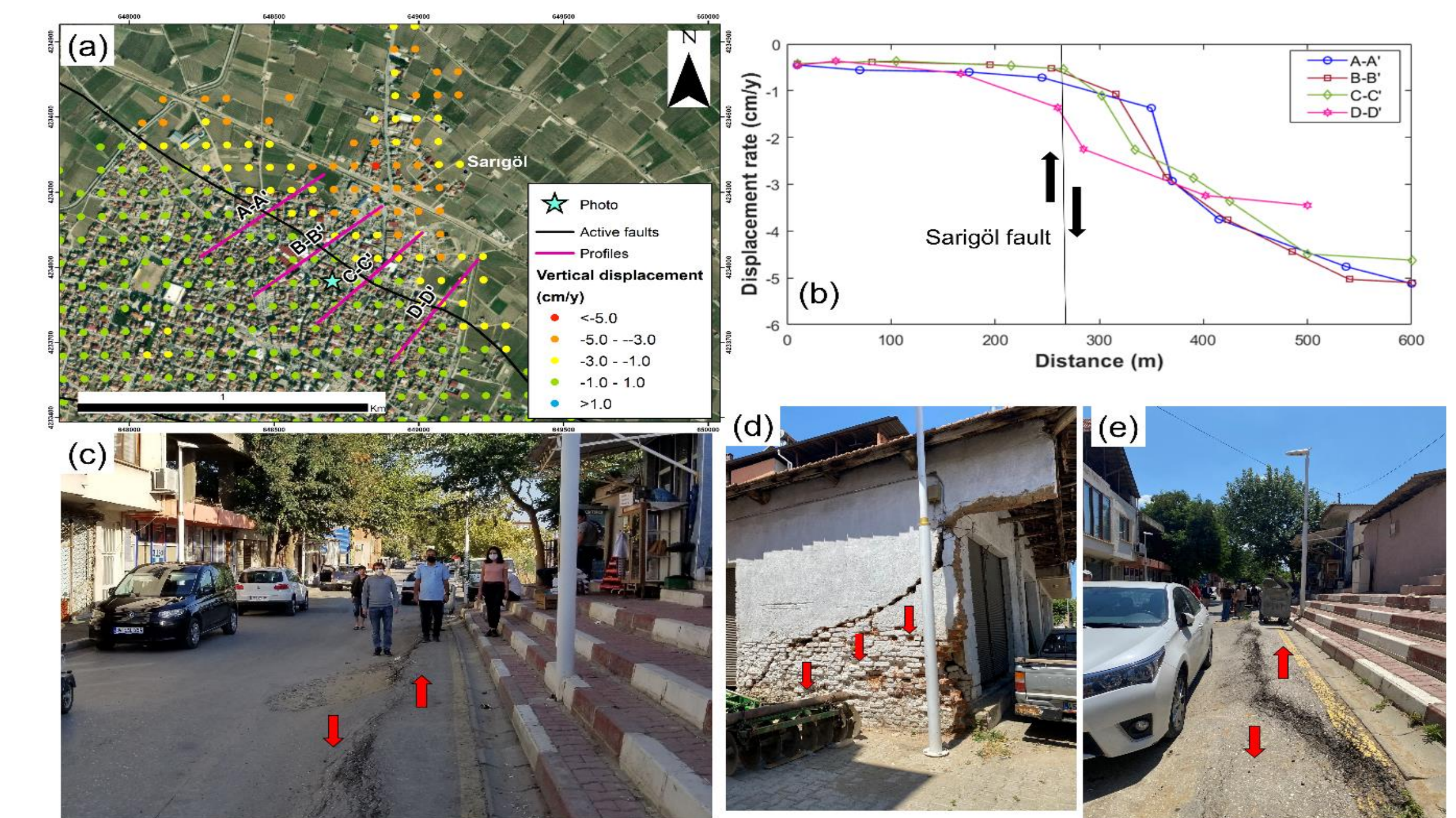

Figure 7. Relationship between active faults and land subsidence: (a) Rate displacement map covering Sarıgöl fault influence area. (b) Analysis of vertical displacement sections A-A', B-B', C-C' and D-D' along the Sarıgöl fault trace, (c), (d) and (e) Structural damages caused by the displacements in the town of Sarıgöl.

Conclusions

DInSAR results exhibit a direct relationship with soft soil thickness. Additionally, there is a relationship between the piezometric drop and the subsidence in those areas in which high groundwater depletion overlays areas of high soft soil thickness. ICA results reveal two types of spatiotemporal deformation trends captured by the two first components: a) IC1, which corresponds to long term and quasi-linear deformation due to the compaction of the aquitard, and b) IC2 which represents the long-term deformations with seasonal rebounds produced by the seasonal loading and unloading cycles due to water level fluctuations.

References

Herrera-García, G., Ezquerro, P., Tomas, R., Béjar-Pizarro, M., López-Vinielles, J., Rossi, M., Mateos, R. M., Carreón-Freyre, D., Lambert, J., Teatini, P., Cabral-Cano, E., Erkens, G., Galloway, D., Hung, W. C., Kakar, N., Sneed, M., Tosi, L., Wang, H., & Ye, S. (2021). Mapping the global threat of land subsidence. Science, 371(6524), 34–36. https://doi.org/10.1126/science.abb8549

Sadeghi, Z., Wright, T. J., Hooper, A. J., Jordan, C., Novellino, A., Bateson, L., & Biggs, J. (2021). Benchmarking and inter-comparison of Sentinel-1 InSAR velocities and time series. Remote Sensing of Environment, 256(May 2020), 112306. https://doi.org/10.1016/j.rse.2021.112306

Elçi, ., Şimşek, C., Gündüz, O., Baba, A., Acinan, S., Yıldızer, N., & Murathan, A. (2015). Simulation of Groundwater Flow in the Gediz River Basin. EWRA 9th World Congress, June, 1–12. https://doi.org/10.13140/RG.2.1.4694.6404

Duru, B., Yargıcı, A. F., Topçu, C., Çakmak, Ö., Gültekin, O. Ş., Bulut, O. F., Dilek, F. B., & Yetiş, Ü. (2018). Management of Groundwater Quality and Quantity: Gediz River Basin Pilot Study. Turkish Journal of Water Science and Management, 2(2), 84–109. https://doi.org/10.31807/tjwsm.423465

For more info: